A dynamical link between the Arctic and the global climate system

K. Dethloff,[1] A. Rinke,[1] A. Benkel,[2] M. Køltzow,[3] E. Sokolova,[1] S. Kumar Saha,[1] D. Handorf,[1] W. Dorn,[1] B. Rockel,[2] H. von Storch,[2] J. E. Haugen,[3] L. P. Røed,[3] E. Roeckner,[4] J. H. Christensen,[5] and M. Stendel[5]

Received 16 November 2005; revised 12 December 2005; accepted 15 December 2005; published 1 February 2006.

[1] By means of simulations with a global coupled AOGCM it is shown that changes in the polar energy sink region can exert a strong influence on the mid- and high-latitude climate by modulating the strength of the mid-latitude westerlies and storm tracks. It is found, that a more realistic sea-ice and snow albedo treatment changes the ice-albedo feedback and the radiative exchange between the atmosphere and the ocean-sea-ice system. The planetary wave energy fluxes in the middle troposphere of mid-latitudes between 30 and 50°N are redistributed, which induces perturbations in the zonal and meridional planetary wave trains from the tropics over the mid-latitudes into the Arctic. It is shown, that the improved parameterization of Arctic sea-ice and snow albedo can trigger changes in the Arctic and North Atlantic Oscillation pattern with strong implications for the European climate. **Citation:** Dethloff, K., et al. (2006), A dynamical link between the Arctic and the global climate system, *Geophys. Res. Lett.*, *33*, L03703, doi:10.1029/2005GL025245.

1. Introduction

[2] The Arctic region is one of the key areas for understanding how climate might change in the future, because it is where the powerful ice-albedo feedback mechanism operates as discussed by *Curry et al.* [1995] and *Holland and Bitz* [2003]. This feedback is the most important factor for the polar amplification of global warming, summarised by *ACIA* [2005]. Possible future changes in Arctic sea-ice cover and thickness, and consequently changes in the ice-albedo feedback, represent one of the largest uncertainties in the prediction of future temperature change. Variability in the Arctic and polar amplification and feedbacks are recurrent themes in numerical climate modeling but our knowledge of the mechanisms supposed to underpin this link is weak as shown by *Moritz et al.* [2002].

[3] Biases and across-model scatter are present in simulations of Arctic sea-ice, either in the radiative forcing, or in the parameterizations of surface melt and its influence on the absorption of shortwave radiation [*Flato et al.*, 2004]. Main causes of the interannual variability of the sea- ice cover in the Arctic are the year-to-year variations in the atmospheric fields of wind and temperature due to the high sensitivity of the Arctic sea-ice cover to atmospheric forcing as discussed by *Arfeuille et al.* [2000]. Sea-ice introduces additional feedbacks into the coupled climate system, making climate naturally more variable in polar regions. Surface albedo has long been recognized as one of the key surface parameters in climate models through its direct effect on the energy balance. By means of simulations with a global coupled AOGCM we investigate the influence of a more realistic sea-ice and snow albedo treatment changes on the energy balance and atmospheric circulation patterns.

2. Improved Arctic Sea-Ice and Snow Albedo Treatment and the Global Model Set Up

[4] We report on global atmospheric feedbacks arising from the Arctic and connected with reductions or increases in the sea-ice and snow cover, which introduces changes in large-scale atmospheric wave patterns and storm tracks. To look for feedbacks between regional Arctic climate processes and the global climate system, the atmosphere-ocean general circulation model (AOGCM) ECHO-G described by *Zorita et al.* [2004] has been applied with improved sea-ice- and snow albedo feedbacks. The improved snow albedo uses a surface temperature dependent scheme and distinguishes between forested and non-forested areas, while the new sea-ice albedo scheme takes into account snow, pure sea ice, melt ponds and depends on snow cover and surface temperature. Both schemes have been described by *Køltzow et al.* [2003]. These parameterizations lead to a better agreement of the simulated albedo with the Advanced Very High Resolution Radiometer (AVHRR) polar pathfinder [*Xiong et al.*, 2002] as well as with the Surface Heat Budget of the Arctic Ocean (SHEBA) data [*Uttal et al.*, 2002]. The improved sea-ice and snow albedo formulation have been implemented in the regional climate model HIRHAM [*Dethloff et al.*, 2004; *Rinke et al.*, 2004]. The new scheme gives a higher and more realistic albedo in winter and early spring, leading to improved Arctic surface air temperatures compared to the climatological data set of *Willmott and Rawlins* [1999].

[5] The improved and validated Arctic sea-ice and snow albedo parameterizations have been introduced for present-day forcing conditions into the ECHO-G model and unforced simulations over 500 years with fixed present-day greenhouse gases concentrations have been carried out. To analyse the fast atmospheric response to sea-ice and snow albedo changes, not contaminated by the complex feedbacks within the coupled atmosphere-ocean-sea-ice system operating on longer decadal time scales, the first

[1]Research Unit Potsdam, Alfred Wegener Institute for Polar and Marine Research, Potsdam, Germany.
[2]GKSS Research Center, Institute of Coastal Research, Geesthacht, Germany.
[3]Norwegian Meteorological Institute, Oslo, Norway.
[4]Max Planck Institute for Meteorology, Hamburg, Germany.
[5]Danish Meterorological Institute, Copenhagen, Denmark.

0094-8276/06/2005GL025245$05.00

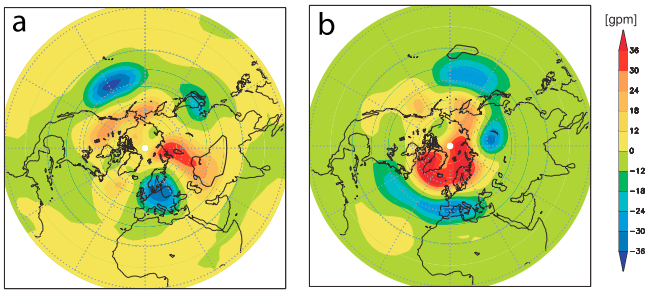

Figure 1. Geopotential difference (gpm) at 500 hPa "New sea-ice and snow albedo run minus control run" averaged over 8 winter (DJF) for two different initial states: (a) (C_NSS-C) and (b) (H_NSS-H). Thick black contours describe the 95% significance level.

9 years of the simulations over 500 years have been analysed. Since the adpatation of the sea-ice cover takes approximately one year, we neglected this year and analysed the eight years 2 to 9. The averaged annual surface air temperature difference between the new sea-ice and snow albedo (C_NSS) run and the control (C) run for this time slice is characterized by a cooling of the Arctic regions as a result of the increased albedo and a warming in a zonal belt covering the mid-latitudes. The annual cycle of Arctic sea-ice extent is found to be more realistic. The reason for the colder temperatures in the Arctic is, that the polar vortex tends to be situated downstream of the northern Rocky Mountains. This preferred location is related to orographic forcing of planetary waves.

3. Atmospheric Changes Following the Improved Sea-Ice and Snow Albedo Scheme

[6] Examining the 500 hPa winter geopotential differences between the C_NSS-run and the C-run in Figure 1a, pronouced changes over high and middle latitudes are recognized, but only a few of them over Eurasia are statistically significant. The influence of an entirely different atmospheric initial state has been investigated in an H_NSS-run, which used different atmospheric initial

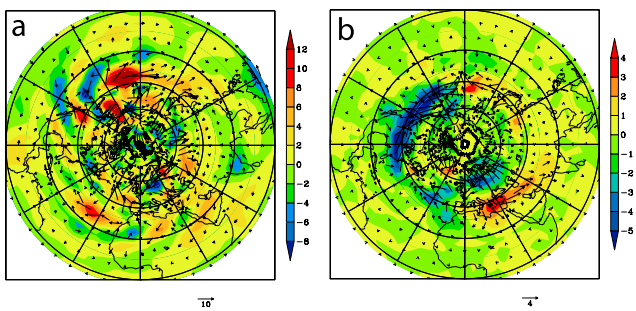

Figure 2. Localised Eliassen-Palm flux differences (m^2s^{-2}) between the "New sea-ice and snow albedo run and the control run" (C_NSS-C) at 500 hPa, averaged over 8 winter (DJF). (a) Low-pass filtered (10–90 days), basic length of 10 m^2s^{-2} and (b) High-pass filtered (2–6 days), basic length of 4 m^2s^{-2}. Colours display the magnitude of the differences; the arrows describe the differences in the EP vector propagation.

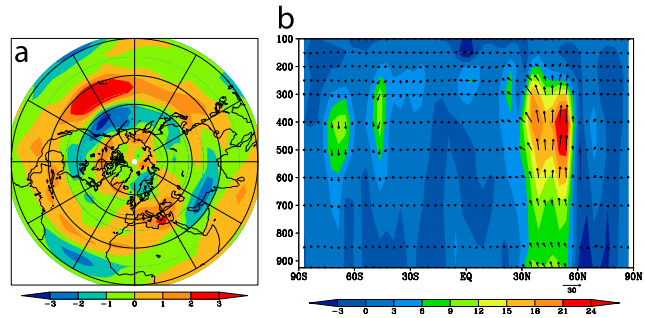

Figure 3. (a) Zonal wind component differences (ms^{-1}) "New sea-ice and snow albedo run and the control run" (C_NSS-C) at 500 hPa, averaged over 8 winter (DJF). (b) Zonally averaged Eliassen-Palm flux differences (10^6 m^3s^{-2}) between the "New sea-ice and snow albedo run and the control run" (C_NSS-C), time scales 10–90 days, averaged over 8 winter (DJF). Pressure coordinate in hPa. Colours display the magnitude of the differences; the arrows describe the differences in the EP vector propagation.

conditions but identical oceanic ones compared to the C_NSS-run. Figure 1b shows the geopotential differences between the H_NSS-run and the H-run. The NSS scheme used with different atmospheric initial conditions always leads to a geopotential increase over the Arctic and a decrease in a mid-latitude belt surrounding the Arctic in agreement with *Deser et al.* [2004].

[7] This simulated large scale and fast response is connected with changes in the planetary wave patterns. These have been analysed by using the localised Eliassen Palm (EP) fluxes diagnosing the wave trains between the tropics and the Arctic and the zonally averaged EP fluxes in the tropo- and stratosphere. The method proposed by *Trenberth* [1986] is a diagnostics of the impact of transient eddies on the time mean flow. Monitoring the energy growth in the dominant modes provides insights into the large-scale dynamical processes that control the model response to changes in the Arctic sea-ice and snow albedo.

[8] Figure 2a presents the differences between the C_NSS and C-run in the low-pass (10–90 days) filtered barotropic part of the EP fluxes at 500 hPa and winter. A pronounced quasi-stationary planetary wave train over the Pacific Ocean occurs propagating south-eastward along the west side of the Rocky Mountains. A weaker wave train is visible over the Atlantic Ocean. The feedback of the sea-ice and snow cover upon the atmospheric circulation is stronger in the Pacific sector than in the Atlantic. Changes in the Arctic energy sink generate a large-scale wave train with centers along the Rocky Mountains. This has been attributed by *Honda et al.* [1996] to the excitation of stationary Rossby waves.

[9] The changes in the large-scale planetary wave trains are accompanied by changes in the storm track activity on time scales of 2–6 days. Figure 2b displays that, strongest changes occur over the North-American continent. Increased storm track activity occurs over the southern part of Greenland and the Fram Strait. The reduced storm track activity over the North Atlantic splits into two parts. One enters Northern Europe and decreases over Scandinavia, the other propagates to North Africa.

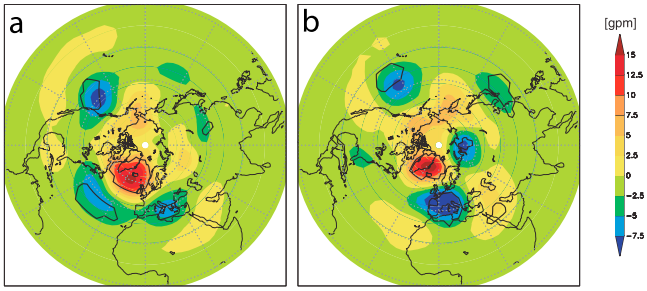

Figure 4. Winter (DJF) geopotential difference (gpm) at 500 hPa "New sea-ice and snow albedo run minus control run" (C_NSS-C) (a) averaged over the first 250 years of the 500 year long run and (b) averaged over the last 250 years of the 500 year long run. Thick black contours describe the 95% significance level.

[10] The wave like disturbances induced by the NSS parameterization are visible in the 500 hPa zonal wind component differences between the C_NSS-run and the C-run shown in Figure 3a. A zonal symmetric pattern with wavelike positive and negative wind anomalies is excited as a result of the improved sea-ice and snow albedo parameterization in the Arctic, disturbed by the high orographic obstacles in the Himalaya region. Figure 3b shows the additional eddy heat and momentum fluxes of the troposphere expressed by the zonally averaged Eliassen-Palm flux differences between the C_NSS and the C-run on seasonal time scales 10–90 days. Maxima occur between 900 and 300 hPa in the latitudinal belt 30–50°N due to the large-scale planetary waves triggered by the NSS scheme. In all other regions of the Northern hemisphere there is a reduction of the atmospheric EP fluxes. A weak remote influence in the mid-troposphere of the Southern hemisphere can be seen. A very similar pattern was obtained for the H_NSS run with the different atmospheric initial state H (not shown), discussed in Figure 1b.

[11] These results indicate that Arctic changes connected with sea-ice and snow cover changes induce significant anomalies in dynamical fields connecting the Arctic and tropical-mid latitudes through meridional and zonal planetary wave guides during winter. Arctic sea-ice and land surface snow perturbations can disturb the atmospheric wave propagation pathways between the Arctic and the tropics in the middle troposphere and in the latitudinal belt between 30 and 50°N. On interannual time scales, the Arctic sea-ice cover is modulated by El Niño/Southern Oscillation events and the response of sea-ice varies for different regions shown by *Liu et al.* [2004].

[12] These results provide a physical explanation how regional sea-ice or snow anomalies in the Arctic can influence the stationary planetary waves and transient storm tracks on a hemispheric and seasonal to inter-annual time scales. On centennial time scales additional feedbacks between the atmospheric and oceanic circulation and the sea-ice cover develop. Therefore the 500 hPa winter geopotential differences between the C_NSS simulations and the C-run have been examined over the whole 500-year-long simulations. Figure 4a shows the 500 hPa geopotential differences between the C_NSS and the C-run, averaged over the first 250 years of the 500 year long run. Strongest differences occur over the whole northern hemisphere, which are statistically significant over the Pacific and the Atlantic Ocean, parts of the Arctic Ocean and the Mediterranian Sea. The difference pattern shows a strong similarity with the Arctic Oscillation (AO) pattern described by *Thompson and Wallace* [1998] and reveal a clear hint on triggering a North Atlantic Oscillation (NAO) like pattern, partly visible already in Figure 1b.

[13] Figure 4b shows the geopotential differences over the last 250 years of the 500 year long run. The AO/NAO like patterns persist also over the second 250 years interval with some shifts in the main centers of action over the Pacific ocean and the Atlantic ocean and Mediterranian sea. These shifts are a result of the non-stationarity of the AO/NAO pattern and could be connected with changes in the oceanic circulation. The circulation differences which results from the NSS simulations, project on the existing natural circulation modes of the climate system and trigger changes in the AO/NAO pattern with strong implications for the European climate.

4. Conclusions

[14] Changes in the polar energy sink region exert a strong influence on the mid- and high-latitude climate by modulating the strength of the sub-polar westerlies and storm tracks. Disturbances in the wintertime Arctic sea-ice and snow cover induce perturbations in the zonal and meridional planetary wave train from the tropics over the mid-latitudes into the Arctic. This approves, that Arctic processes can feed back on the global climate system via an atmospheric wave bridge between the energy source in the tropics and the energy sink in the polar regions. The atmospheric heat and momentum fluxes on seasonal time scales increase in the middle and high troposphere between 30 and 50 °N as a result of the new sea-ice and snow albedo parameterization of the Arctic. The improved parameterisation of Arctic sea-ice and snow albedo in a global climate model exert strong influences on the global geopotential pattern of the middle troposphere and shows similarities with the Arctic Oscillation and North Atlantic Oscillation patterns.

[15] **Acknowledgments.** This work was carried out as part of the EU 5th Framework project GLIMPSE (Global implications of Arctic climate processes and feedbacks) under contract EVK2-CT-2002-00164. We thank Ib Troen and Georgios Amanatidis for support and two anonymous reviewers for constructive comments.

References

ACIA (2005), *Arctic Climate Impact Assessment*, 1042 pp., Cambridge Univ. Press, New York.

Arfeuille, G., L. A. Mysak, and L.-B. Tremblay (2000), Simulation of the inter-annual variability of the wind-driven Arctic sea-ice cover during 1958–1998, *Clim. Dyn.*, *16*, 107–121.

Curry, J. A., J. Schramm, and E. E. Ebert (1995), On the sea-ice albedo climate feedback mechanism, *J. Clim.*, *8*, 240–247.

Deser, C., G. Magnusdottir, R. Saravanan, and A. Phillips (2004), The effects of North Atlantic SST and sea ice anomalies on the winter circulation in CCM3. part II: Direct and indirect components of the response, *J. Clim.*, *17*, 877–889.

Dethloff, K., W. Dorn, A. Rinke, K. Fraedrich, M. Junge, E. Roeckner, V. Gayler, U. Cubasch, and J. H. Christensen (2004), The impact of Greenland's deglaciation on the Arctic circulation, *Geophys. Res. Lett.*, *31*, L19201, doi:10.1029/2004GL020714.

Flato, G. M., and Participating CMIP Modelling Groups (2004), Sea-ice and its response to CO_2 forcing as simulated by global climate models, *Clim. Dyn.*, *23*, 229–241.

Holland, M. M., and C. M. Bitz (2003), Polar amplification of climate change in the coupled model intercomparison project, *Clim. Dyn.*, *21*, 221–232.

Honda, M., K. Yamazaki, Y. Tachibana, and K. Takeuchi (1996), Influence of Okhotsk sea-ice extent on atmospheric circulation, *Geophys. Res. Lett.*, *23*, 3595–3598.

Køltzow, M. Ø., S. Eastwood, and J. E. Haugen (2003), Parameterization of snow and sea-ice albedo in climate models, *Res. Rep. 149*, Norw. Meteorol. Inst., Oslo.

Liu, J., J. A. Curry, and Y. Hu (2004), Recent Arctic sea ice variability: Connections to the Arctic Oscillation and the ENSO, *Geophys. Res. Lett.*, *31*, L09211, doi:10.1029/2004GL019858.

Moritz, R. E., C. M. Bitz, and E. J. Steig (2002), Dynamics of recent climate change in the Arctic, *Science*, *297*, 149–151.

Rinke, A., K. Dethloff, and M. Fortmann (2004), Regional climate effects of Arctic Haze, *Geophys. Res. Lett.*, *31*, L16202, doi:10.1029/2004GL020318.

Thompson, D. W. J., and J. M. Wallace (1998), The Arctic Oscillation signature in the wintertime geopotential height and temperature fields, *Geophys. Res. Lett.*, *25*, 1297–1300.

Trenberth, K. E. (1986), An assessment of the impact of transient eddies on the zonal flow during a blocking episode using localized Eliassen-Palm flux diagnostics, *J. Atmos. Sci.*, *43*, 2070–2087.

Uttal, T., et al. (2002), Surface heat budget of the Arctic Ocean, *Bull. Am. Meteorol. Soc.*, *83*, 255–275.

Willmott, C. J., and M. A. Rawlins (1999), Arctic land-surface air temperature: Gridded monthly and annual climatologies (version 1.01), Cent. for Clim. Res., Dep. of Geogr., Univ. of Del., Newark.

Xiong, X., K. Stammes, and D. Lubin (2002), Surface albedo over the Arctic Ocean derived form AVHRR and its validation with SHEBA data, *J. Appl. Meteorol.*, *41*, 413–425.

Zorita, E., et al. (2004), Climate evolution in the last five centuries simulated by an atmosphere-ocean model: Global temperatures, the North Atlantic Oscillation and the Late Maunder Minimum, *Meteorol. Z.*, *13*, 271–289.

A. Benkel, B. Rockel, and H. von Storch, GKSS Research Center, Institute of Coastal Research, Max-Planck-Strasse 1, PO Box, D-21502 Geesthacht, Germany.

J. H. Christensen and M. Stendel, Danish Meterorological Institute, Lyngbyvej 100, DK-2100 Copenhagen O, Denmark.

K. Dethloff, W. Dorn, D. Handorf, S. Kumar Saha, A. Rinke, and E. Sokolova, Research Unit Potsdam, Alfred Wegener Institute for Polar and Marine Research, D-14473 Potsdam, Telegrafenberg A43, Germany. (dethloff@awi-potsdam.de)

J. E. Haugen, M. Køltzow, and L. P. Røed, Norwegian Meteorological Institute, P.O. Box 43, Blindern, N-0313 Oslo, Norway.

E. Roeckner, Max Planck Institute for Meteorology, Bundesstrasse 55, D-20146 Hamburg, Germany.